Neutron capture cross section of ^{15}N at stellar energies

J. Meissner, H. Schatz, H. Herndl,* and M. Wiescher
Department of Physics, University of Notre Dame, Notre Dame, Indiana 46556

H. Beer and F. Käppeler
Forschungszentrum Karlsruhe, Institut für Kernphysik III, P.O. Box 3640, D–76021 Karlsruhe, Germany
(Received 3 October 1995)

The neutron capture rate on ^{15}N may be of considerable importance for *s*-process nucleosynthesis in red giants as well as for the nucleosynthesis in inhomogeneous big bang scenarios. We measured the reaction cross section of ^{15}N$(n,\gamma)^{16}$N at the Forschungszentrum Karlsruhe with a fast cyclic neutron activation technique at laboratory neutron energies of 25, 152, and 370 keV. Direct capture and shell model calculations were performed to interpret the results. The presented reaction rate is 30–50 % smaller than the previously used theoretical rates.

PACS number(s): 25.40.Lw, 26.20.+f, 26.35.+c

I. INTRODUCTION

Neutron capture reactions on light nuclei may be of considerable importance for the *s*-process nucleosynthesis in red giant stars as well as for the nucleosynthesis in inhomogeneous big bang scenarios. To determine the reaction rates for such different temperature conditions, the cross sections need to be known for a wide energy range.

The reaction ^{15}N$(n,\gamma)^{16}$N represents an important link in the reaction sequences for the production of heavier isotopes in such scenarios. At high temperatures, the cross section for this reaction may be influenced not only by *s*-wave capture but also by nonresonant *p*-wave contributions and by resonances at higher energies. To study these effects and to determine the influence of the various possible contributions, the cross section has been measured for different neutron energies using a fast cyclic activation technique. To supplement the experimental data and to understand the contributions to the stellar reaction rate shell model calculations have been performed and compared to experimentally known parameters.

Throughout this work, all energies are given in the laboratory system, except for resonance energies, which are given in the center of mass system.

II. EXPERIMENTAL METHOD

The experiment was performed at the 3.75 MV Van de Graaff accelerator at the Forschungszentrum Karlsruhe (FZKA). Because of the short half-life of the reaction product ^{16}N ($t_{1/2}=7.13$ s), a fast cyclic activation technique was applied [1] to measure the (n,γ) cross section of ^{15}N at different neutron energies.

Neutrons were generated via the ^{7}Li$(p,n)^{7}$Be reaction at proton energies between 1.912 and 2.14 MeV using metallic lithium targets. At the lowest proton energy of 1.912 MeV,

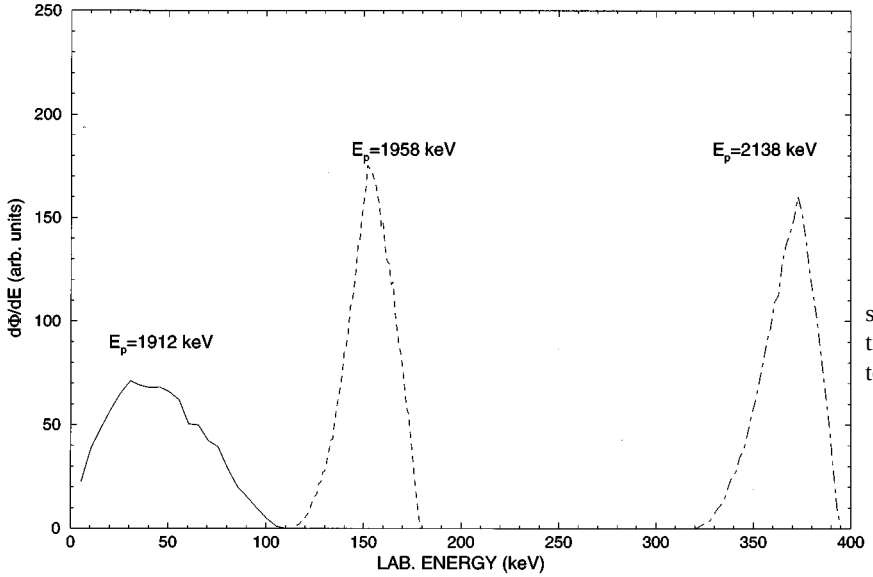

FIG. 1. The Monte Carlo simulated neutron spectra were generated using the ^{7}Li(p,n) reaction cross sections at the respective indicated proton energies.

*Present address: Technische Universität Wien, A–1040 Wien, Austria.

TABLE I. Sample characteristics and experimental cross sections.

$\bar{E}_n$ (keV)[a]	Sample mass ^{197}Au (mg)	Sample mass ^{nat}Kr (mg)	Sample mass $^{15}N_2$ (mg)	$\langle d_{sphere}\rangle / \langle d_{foil}\rangle$	^{15}N(n,γ) cross section $\langle\sigma\rangle$ (μb)[b]	^{15}N(n,γ) cross section $\sigma(\bar{E}_n)$ (μb)[c]
25		211.6	57.4		5.63±0.73	
		224.1	892.7		4.87±0.44	
		224.1	892.7		5.08±0.46	
		224.1	892.7		4.94±0.49	
		224.1	892.7		6.26±0.47	
25		weighted average			5.32±0.46[d]	3.5±0.47
152	169.2		892.7	102.6±12	11.3±1.5	10.8±1.5
370	163.5		892.7	82.5±10	18.4±2.6	18.1±2.6

[a]Mean neutron energy.
[b]Averaged cross section.
[c]Unfolded experimental cross section.
[d]Error does not include the 7% uncertainty of the ^{86}Kr(n,γ) cross section.

just above the neutron threshold, the angle integrated neutron spectrum obtained from a thick Li target resembles a Maxwell-Boltzmann distribution at a thermal energy of $kT=25$ keV [2,3]. At higher energies, thin Li targets were used to produce narrow neutron spectra. Time-of-flight measurements were taken with a ^{6}Li glass detector located at an angle $\theta=0°$ and a distance of 93 cm from the neutron target. Based on this measurement the true neutron spectrum in the solid angle range of the activated sample was calculated by a Monte Carlo simulation (for details see Ref. [4]). The resulting spectra have widths of 22 and 30 keV at the investigated neutron energies of 152 and 370 keV and are shown in Fig. 1.

The samples consisted of a mixture of natural krypton and $^{15}N_2$ (enriched to 99.7%) gas. This mixture was confined in stainless steel spheres with an inner diameter of 19 mm and a wall thickness of 0.5 mm. The sample masses were determined to better than ±1 mg by weighing the sphere during the various steps of filling with krypton and nitrogen (for details see Ref. [5]). Typical pressures in the stainless steel spheres at room temperature were calculated to be between 3 Mpa and 21 Mpa. Table I shows the sample masses in detail.

After irradiation, the ^{15}N$(n,\gamma)^{16}$N cross section was determined from the induced γ activities. The ^{16}N activity was obtained via the measurement of the γ ray from the 6.130 MeV ($J^\pi=3^-$) to ground state transition in ^{16}O. This level is populated with 66.2% probability in the β^- decay of ^{16}N [6]. For the 25 keV runs, the ^{15}N cross section was measured relative to the (n,γ) cross section of ^{86}Kr, which has been determined independently using the same setup and neutron spectrum [5]. At higher neutron energies, the ^{86}Kr cross section is too small to yield a sufficient γ activity. Instead, the cross section was measured relative to the well known (n,γ) cross section of ^{197}Au [3] by irradiating gold foils in front of the gas samples. The decay properties of the respective product nuclei are summarized in Table II.

Because of the short half-life of ^{16}N, cyclic neutron irradiations were carried out with a fast sample changer [7], which moved the samples repeatedly between the irradiation and counting positions. The irradiation time t_b and the counting time t_c were set to 14 s, roughly two half-lives of ^{16}N. The transition time between irradiation and counting positions was measured and is $t_w=0.4$ s. At the counting position, the decay of the product nuclei was observed with a well shielded 35% HPGe detector (2 keV resolution at 1.3 MeV). During the counting time, the proton beam was blocked in order to avoid excessive backgrounds. The accumulated γ-ray spectrum of an activation at $E_n=25$ keV is shown in Fig. 2. It should be noted that the spectrum is not linear in energy. This does not affect the peak intensities. All indicated γ-ray energies are in keV.

Two different ^{15}N samples (see Table I) were used for five activations at $\bar{E}_n=25$ keV relative to the ^{86}Kr cross section [5] and two activations were performed at 152 and 370 keV relative to the ^{197}Au cross section [3]. The activities of the gold samples were measured with the same detector and in the same counting position as for the gas sample after the activation ended. The difference for the mean path length in the spherical gas and the flat gold sample required a correction that was calculated by a Monte Carlo simulation [4]. This correction is indicated by the ratio $\langle d_{sphere}\rangle/\langle d_{foil}\rangle$ in Table I.

The experimental procedure and the related data analysis are described in detail in Ref. [4], where this setup was used for a measurement of the ^{18}O cross section. The neutron averaged cross sections are listed in Table I and the excitation curve is shown in Fig. 3.

III. RESULTS

A. Nonresonant contributions

To evaluate the experimental data calculations of the p wave direct capture cross section were performed in terms of

TABLE II. Decay properties of the relevant product nuclei.

Product nucleus	Half-life	γ-ray energy E_γ (keV)	Relative intensity per decay, I_γ (%)
^{16}N	7.13±0.02 s	6130	66.2±0.6[a]
^{87}Kr	1.27±0.01 h	407	49.6±2.0[b]
^{198}Au	2.696±0.002 d	412	95.5±0.1[c]

[a]Reference [6].
[b]Reference [5].
[c]Reference [17].

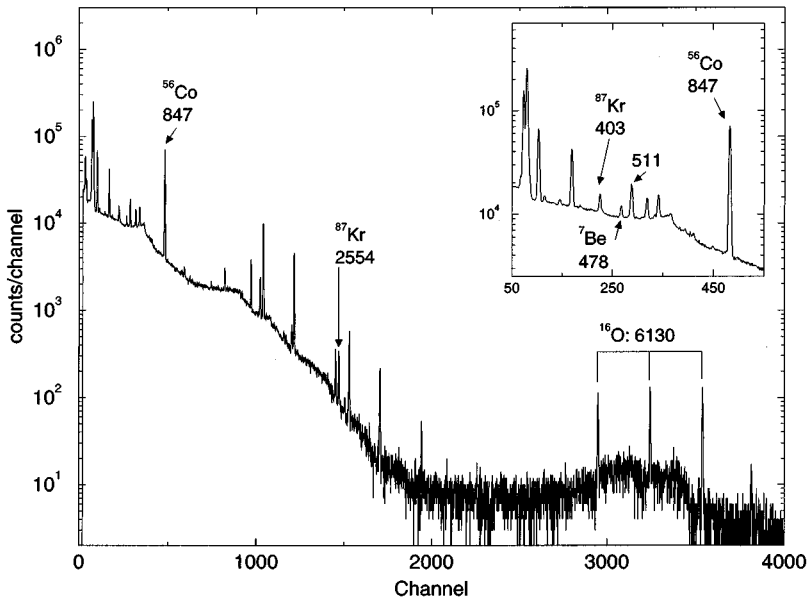

FIG. 2. One of the ^{16}N and ^{87}Kr activation spectra at $E_n = 25$ keV (γ-ray energies are given in keV; see text).

a nuclear potential model using a Wood-Saxon potential for the final state wave function [8]. In this calculation, the experimentally determined spectroscopic factors from Ref. [9] for the ground state and the first three excited states, $C^2S =$ 0.55, 0.46, 0.54, and 0.52, were adopted, respectively (see Tables III and IV). The authors of Ref. [9] quote 30% uncertainty for their spectroscopic factors. The resulting p-wave direct capture cross section is mainly $\sqrt{E}$ dependent [10,8]. However, at higher neutron energies the p-wave penetrability deviates from the pure $\sqrt{E}$ dependency and we chose the parametrization to be

$$\sigma_{\mathrm{DC}}(E) = A\sqrt{E} - BE^{1.2}. \quad (1)$$

The exponent of the correction term results from a fit to the calculated cross section. For the present study $A = 29\ \mu$b MeV$^{-1/2}$ and $B = 12\ \mu$b MeV$^{-1.2}$ have been extracted for the sum of all direct capture contributions. The strongest contribution originates from the p wave capture to the excited state at 0.397 MeV (see Table III). For comparison to the experiment, we folded the calculated direct capture cross section with the Monte Carlo simulated shape of the neutron spectra. Figure 3 shows the excellent agreement of the presented experimental cross sections in comparison with the direct capture calculations. It should be noted that the uncertainty in the calculated cross section due to the spectroscopic factors (30%) is not shown in the figure.

B. Level parameters in ^{16}N

As the magnitude of the cross section is directly correlated with the spectroscopic factors of the ground state and the first few excited states we also performed shell model calculations with the computer code OXBASH [11] for comparison. The ground state and first three excited states of ^{16}N have spins 0^-, 1^-, 2^-, and 3^- and can be well explained with a $2s_{1/2}$ and a $1d_{5/2}$ neutron coupling to the $1/2^-$ ground state of ^{15}N (resulting in a 0^- and 1^- state in

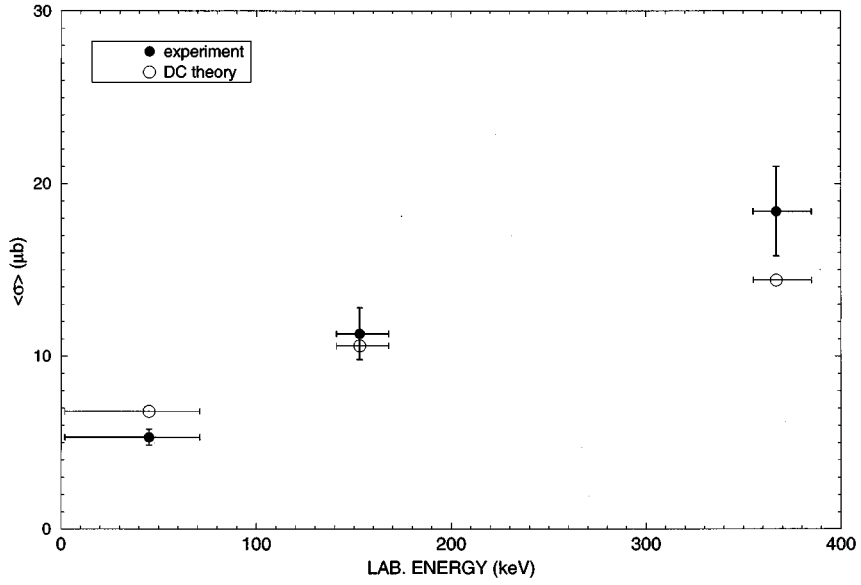

FIG. 3. Excitation curve of ^{15}N$(n,\gamma)^{16}$N. The experimental data (black circles) represent the mean cross section integrated over the neutron energy distribution. The open circles represent the calculated total direct capture cross section integrated over the respective neutron spectrum. The main uncertainty in the calculated cross section arises from the uncertainty of the spectroscopic factors (30%).

TABLE III. Parameters for the direct capture (DC) contributions (see text).

DC→	Transition	C^2S[a]	A[b]	B[b]
0.000 MeV	$p\rightarrow d$	0.55	2.32	0.55
0.120 MeV	$p\rightarrow s$	0.46	5.6	2.5
0.296 MeV	$p\rightarrow d$	0.54	2.87	0.65
0.397 MeV	$p\rightarrow s$	0.52	18.5	8.5
Sum			29.3	12.2

[a]The spectroscopic factors have uncertainties of ±30% (see Ref. [9]).
[b]Parameters A and B are extracted from a fit of Eq. (1) to the calculated DC cross section.

the first case and a 2^- and 3^- state in the second). Therefore these states are good single particle states and their spectroscopic factors should be close to unity. In a shell model calculation of the spectroscopic factors the interaction ZBMI of [12] was used, assuming a closed ^{12}C core and populating the shells $1p_{1/2}$, $1d_{5/2}$, and $2s_{1/2}$. Since no restrictions were imposed the calculation included also particle-hole excitations from the p into the sd shell. The spectroscopic factors are still close to unity which would be the result in a pure single particle picture (see Table IV).

It should be noted that the shell model predictions for the spectroscopic factors are off by a factor of 2 compared to the experimental results [9] in the case of ^{15}N+n (see Table IV). It is not clear why the shell model predictions disagree with the experimental spectroscopic factors in Ref. [9].

The known resonance at $E_R^{\text{c.m.}}=862$ keV may contribute to the reaction rate at higher temperatures. Its experimental total width $\Gamma=15$ keV [13,14] corresponds to the neutron partial width of the corresponding state. The resonance strength depends, therefore, only on the partial width of the γ channel, Γ_γ:

TABLE IV. Comparison of previous experimental data with shell model predictions.

E_x (MeV) Expt.	J^π	l_f	C^2S Expt.[a]	C^2S OXBASH
0	2^-	$1d_{5/2}$	0.55	0.93
0.120	0^-	$2s_{1/2}$	0.46	0.95
0.296	3^-	$1d_{5/2}$	0.54	0.87
0.397	1^-	$2s_{1/2}$	0.52	0.96

[a]From Ref. [9].

$$\omega\gamma=\frac{2J+1}{4}\Gamma_\gamma. \tag{2}$$

The recommended upper limits (RUL's) for the strength of γ-ray transitions [15] were used to calculate the upper limit of the γ partial width. Only $E1$ transistions were considered to the ground state and to the excited states at 0.120 keV ($J^\pi=0^-$) and 0.397 keV ($J^\pi=1^-$). With a RUL of 100 m W.u. (where W.u. is a Weisskopf unit) [15] for $E1$ transistions the γ partial width was calculated to be $\Gamma_\gamma=4.2$ eV. This results in an upper limit of $\omega\gamma\leqslant 3.15$ eV for the resonance strength.

C. Stellar reaction rates

In summary, the stellar rate for the ^{15}N(n,γ) ^{16}N reaction can be parametrized in the temperature range up to $T_9=3$ GK by

$$N_A\langle\sigma v\rangle=3.18+3.27\times10^3T_9-493T_9^{1.7}+5.3\times10^5T_9^{-3/2}$$
$$\times\exp(-10.0/T_9)[\text{cm}^3\ \text{s}^{-1}\ \text{mol}^{-1}],$$

where T_9 is the temperature in GK. The first three terms represent the s-wave and p-wave capture contributions, respectively. The last term represents the upper limit due to the possible resonance. From Fig. 4 it is evident that the as-

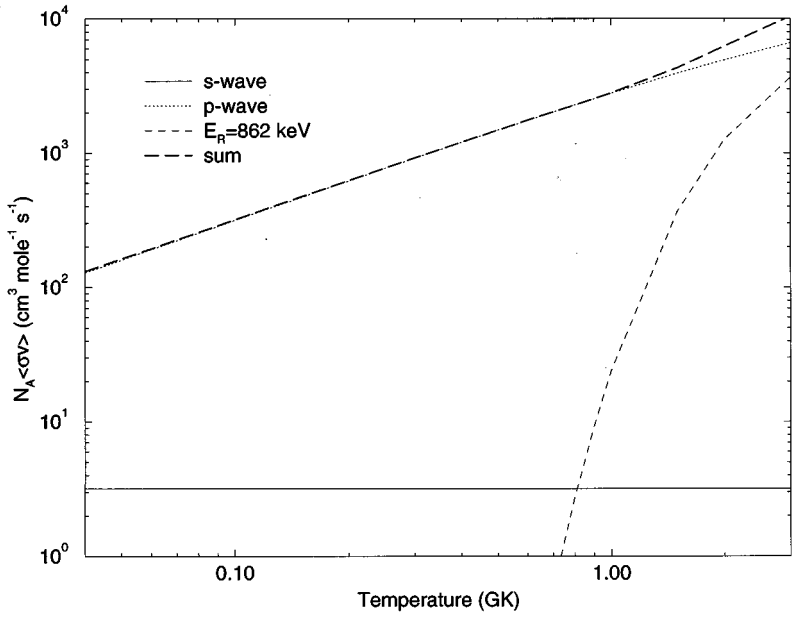

FIG. 4. Reaction rate contributions.

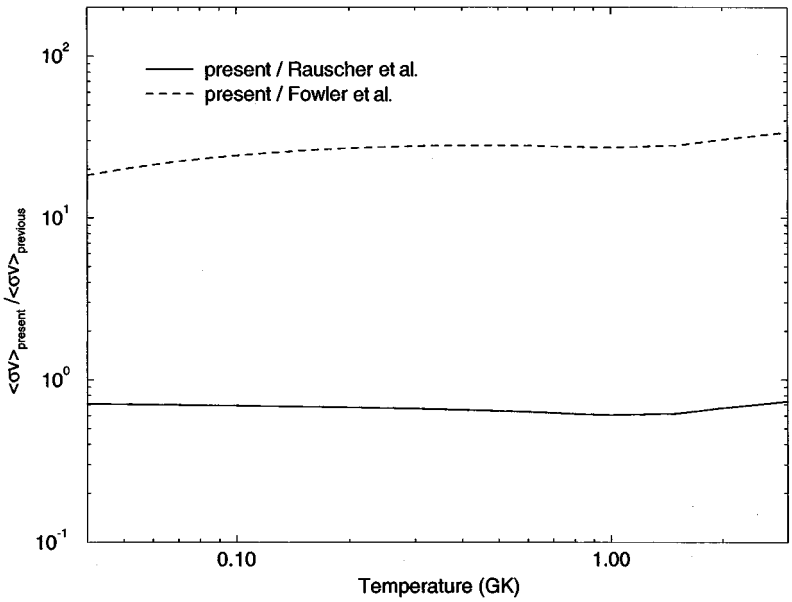

FIG. 5. Comparison of the present reaction rate with previous predictions.

sumed resonance does not play any significant role below temperatures $T_9 < 1$ GK. Above $T_9 = 1$ GK the rate may be influenced up to 50% by the possible resonance at $E_R = 862$ keV. This present reaction rate is 30% to 50% smaller than the theoretical rates previously used by Rauscher *et al.* [10] (see Figs. 4 and 5). This is mainly due to the fact that the observed experimental spectroscopic factors are smaller than the ones predicted by the shell model which were used in Ref. [10]. The rate in Ref. [16] is about 20–30 times smaller than the present result. The previous rate, however, is just a first order estimate of the p-wave capture contribution (see Fig. 5).

ACKNOWLEDGMENTS

We would like to thank G. Rupp for his continuous technical assistance throughout the experiment as well as A. Ernst, E.-P. Knaetsch, D. Roller, and W. Seith for their efforts in providing a reliable operation of the accelerator. This project was partially funded by NSF Grant No. PHY88-03035. J.M. was supported by the National Academy of Science through Sigma Xi, H.S. by the German Academic Exchange Service (DAAD), and H.H. by the ''Fonds zur Förderung der wissenschaftlichen Forschung'' in Vienna, Austria.

[1] H. Beer, G. Rupp, F. Voss, and F. Käppeler, Astrophys J. **379**, 420 (1991).
[2] H. Beer and F. Käppeler, Phys. Rev. C **21**, 534 (1980).
[3] W. Ratynski and F. Käppeler, Phys. Rev. C **37**, 595 (1988).
[4] J. Meissner, H. Schatz, J. Görres, H. Herndl, M. Wiescher, H. Beer, and F. Käppeler, Phys. Rev. C **53**, 459 (1996).
[5] H. Beer, Astrophys. J. **375**, 823 (1991).
[6] D.R. Tilley and H.R. Weller, Nucl. Phys. **A564**, 1 (1993).
[7] H. Beer, G. Rupp, G. Walter, F. Voss, and F. Käppeler, Nucl. Instrum. Methods Phys. Res. Sect. A **337**, 492 (1994).
[8] M. Wiescher, J. Görres, and F.-K. Thielemann, Astrophys. J. **363**, 340 (1990).
[9] W. Bohne, J. Bommer, H. Fucks, K. Grabisch, H. Kluge, and G. Röschert, Nucl. Phys. **A196**, 41 (1972).
[10] T. Rauscher, J.H. Applegate, J.J. Cowan, F.-K. Thielemann, and M. Wiescher, Astrophys. J. **429**, 499 (1994).
[11] B.A. Brown, A. Etchegoyen, W.D.M. Rae, and N.S. Godwin (unpublished).
[12] A.P. Zuker, B. Buck, and J.B. McGrory, Phys. Rev. Lett. **21**, 39 (1968).
[13] F. Ajzenberg-Selove, Nucl. Phys. **A460**, 1 (1986).
[14] *Neutron Cross Sections*, edited by J.F. Mughabghab, M. Divadeenam, and N.E. Holden (Academic Press, New York, 1981), Vol. 1, Pt. A.
[15] P.M. Endt, At. Data Nucl. Data Tables **55**, 171 (1993).
[16] W.A. Fowler, G.E. Caughlin, and B.A. Zimmerman, Annu. Rev. Astron. Astrophys. **5**, 525 (1967).
[17] R.L. Auble, Nucl. Data Sheets **40**, 301 (1983).